Int. J. Electrochem. Sci., 12 **(2017)** 9311 – 9319, doi: 10.20964/2017.10.14

International Journal of
ELECTROCHEMICAL
SCIENCE
www.electrochemsci.org

Electrodeposition of CdS-TiO_2 for the Photocatalytic Degradation of Ammonia-Nitrogen Wastewater

Yong Jing[1,2], *Xiaomin Hu*[1,*] *and Chunyan Shao*[2]

[1] School of Resources and Civil Engineering, Northeastern University, 3-11, Wenhua Rd, Heping, Shenyang, Liaoning, P.R. China
[2] Shenyang Academy of Environmental Sciences, 98, No. 3 Quanyun Rd, Hunnan, Shenyang, Liaoning, P.R. China
[*]E-mail: hxmin_jj@163.com

Received: 10 June 2017 / *Accepted:* 25 July 2017 / *Published:* 12 September 2017

In this work, a simple, one-stage electrodeposition strategy was used to prepare a CdS-nanoparticle-sensitized TiO_2 (CdS-TiO_2) nanotube array. TiO_2 nanotubes sensitized by other narrow-band-gap semiconductors were also prepared using this distinct strategy. The CdS-TiO_2 hybrid exhibited more desirable physical and chemical characteristics for photocatalytic activity with stronger visible-light-response capacity compared with the original TiO_2 material. In comparison with the original TiO_2, CdSe/TiO_2, and CdTe/TiO_2, the catalytic capacity of CdS-TiO_2 to ammonia-nitrogen wastewater was higher. The maximum pH value for the CdS-TiO_2-induced ammonia-nitrogen removal was 10. Nevertheless, inhibition effects on ammonia-nitrogen degradation were exhibited by all common inorganic ions: Mg^{2+}, Ca^{2+}, K^+, Na^+, HCO_3^-/CO_3^{2-}, SO_4^{2-}, NO_3^-, and Cl^-.

Keywords: Ammonia-nitrogen wastewater; Photocatalysis; Electrodeposition; CdS; TiO_2

1. INTRODUCTION

Rare earth metals have recently been increasingly mined in the Gannan area of China, leading to substantial discharge of ammonia-nitrogen wastewater into environmental water sources. Many detrimental impacts could be caused by the excessive ammonia-nitrogen discharge into water, and the treatment of ammonia-nitrogen wastewater has aroused much interest [1]. To treat low concentrations of ammonia-nitrogen wastewater, blow-off, chemical precipitation and adsorption techniques have been extensively used. For blow-off techniques, basic water is obtained using NaOH, leading to the existence of ammonia-nitrogen in the form of NH_3 (free ammonia). Ammonia-nitrogen is difficult to recover after escaping from aqueous solutions into the atmosphere, which would lead to further

atmospheric pollution. Chemical precipitation focuses on the generation of insoluble salts to make ammonia-nitrogen less water soluble. Adsorption refers to a reversible process, where NH_4^+ ions are exchanged with other cationic ions with limited exchange ability [2-4]. The conversion of ammonia-nitrogen into nitrogen is considered an ideal treatment. Marco [5] successfully oxidized partial ammonia-nitrogen into nitrogen with a TiO_2 catalyst using a photocatalytic oxidation strategy.

Photocatalytic oxidation is the most promising potential techniques for water pollutant treatment. This technique has aroused substantial interest and has been extensively studied in the fields of building materials, environmental protection, etc. (typically for pollutant photodegradation) [6-12]. The non-toxicity and desirable stability of photocatalytic oxidation makes it better than other improved oxidation techniques, including electrochemical oxidation, catalytic wet oxidation, ozone oxidation, and Fenton oxidation [13]. Obviously, titanium dioxide (TiO_2) is typically compared with other semiconductor photocatalytic materials, since it is biologically and chemically stable, readily available, photocatalytically active under ultraviolet irradiation, and low cost [14-17]. Nevertheless, it is still limited in utility, since its electron-hole recombination rate is high during photocatalysis. In addition, TiO_2 only absorbs ultraviolet light of $\leq$ 387.5 nm, accounting for *ca.* 4% of sunlight [18-20]. To solve the aforementioned problems, the photoresponse of TiO_2 can be extended to the visible region using previously reported methods [21, 22]. In addition to this approach, the migration efficiency of photogenerated electrons could be increased, and the recombination rate of electron-hole pairs could be decreased by doping certain amounts of metals or nonmetal elements into TiO_2. The photodegradation of ammonia-nitrogen using modified TiO_2 has been proposed in other works [23-26]. Fe-doped TiO_2 used visible-light wavelengths, effectively generating hydrogen through the decomposition of aqueous NH_3. On the other hand, rare-earth-ion-doped TiO_2 is of great importance in the photocatalytic decomposition of ammonia.

In this study, a rapid one-stage electrodeposition strategy was used for the synthesis of a CdS-sensitized TiO_2 nanotube array. Partially embedding CdS nanoparticles into the TiO_2 nanotube shells was achieved by codeposition with TiO_2, which differed from the attachment of CdS nanoparticles to the TiO_2 nanotube surfaces presented in previous works. In addition, a uniform distribution of CdS nanoparticles throughout the TiO_2 nanotubes was observed, as well as the expedient controlling of the distribution density and size of the nanoparticles. The length of the obtained CdS-TiO_2 nanotubes prepared using this strategy was over 30 μm. Compared with typical TiO_2 nanotube arrays, the photocatalytic behaviour of the CdS-TiO_2 nanotube array was much more desirable.

2. EXPERIMENTS

2.1. Chemicals

Sodium sulphide (Na_2S, Sigma-Aldrich, 98%), sodium hydroxide (NaOH, SCRC, 96%), sodium thiosulfate ($Na_2S_2O_3$, SCRC, 99%), cadmium chloride ($CdCl_2$, SCRC, 99%), and titanium fluoride (TiF_4, Alfa Aesar, 98%) were used as received without any further treatment.

2.2. Synthesis of CdS-TiO_2 Nanotube Array

$Na_2S_2O_3$ (0.05 M), $CdCl_2$ (0.1 M) and TiF_4 (0.04 M) were dissolved into deionized water (100 mL) under stirring for 0.5 h to prepare the electrolyte; the pH value was kept at approximately 1.8. The templates were anodic aluminium oxide (AAO) membranes. Based on an SEM measurement, the he channels were ca. 60 μm in length and ca. 250 nm in diameter. A standard three-electrode system (CH instruments, model 620B) was used for the electrodeposition, where the reference and counter electrodes were a saturated Ag/AgCl electrode and a platinum coil, respectively. In addition, the working electrode was prepared by sputtering a Au layer as thin as approximately 40 nm onto the back of an AAO membrane prior to electrodeposition. The AAO membrane was then removed using NaOH (1 M) for 0.5 h at 40 °C after the electrodeposition. Finally, a highly ordered CdS-TiO_2 nanotube array was yielded, which was then annealed under air or argon for 3 h at 500 °C.

2.3. Synthesis of CdSe and CdTe Nanoparticles Sensitized TiO_2 Nanotube Arrays.

SeO_2, $CdSO_4$ and TiF_4 (3 mM, 0.2 M and 0.04 M, respectively) were dissolved into deionized water (100 mL) to prepare the electrolyte for CdSe. The corresponding parameters of the electrodeposition were as follows: time = 20 min, temperature = 60 °C, and potential = -0.6 V. TeO_2, $CdSO_4$ and TiF_4 (CdTe, 1 mM, 0.2 M and 0.04 M, respectively) were dissolved into deionized water (100 mL) to prepare the electrolyte for CdTe. The corresponding parameters of the electrodeposition were as follows: time = 20 min, temperature = 60 °C, and potential = -0.4 V. Although the CdTe- and CdSe-nanoparticle-sensitized TiO_2 nanotube arrays were prepared under various conditions, they were ultimately synthesized using the same procedure as that of the CdS-TiO_2 nanotube array.

2.4. Photocatalytic Removal Experiments and Analytical Methods

A XPA-7 photochemical reactor was used for the photocatalytic degradation tests. A 500 W mercury lamp provided the irradiation, where the wavelength of the light was 365 nm, located in the cylindrical quartz cold trap. Water circulation was used to cool the system, which was kept at ambient temperature. The adsorption equilibria of ammonia-nitrogen on the catalysts were maintained by magnetically stirring the suspension for 0.5 h in the dark prior to irradiation. Irradiation was performed for 300 min in all reactions. The reaction solution (ca. 5 mL) was sampled at certain time intervals, followed by centrifugation. Nessler's reagent spectrophotometry was used to measure the supernatant. In addition, the calculation of the removal efficiency (*R*)is described by Formula (1):

$$R = (C_0 - C) / C_0 \times 100\%$$

where C_0 and C represent the initial concentration of ammonia-nitrogen and the concentration at reaction time t (min), respectively. In addition, NO_3-N and NO_2-N were studied using spectrophotometry to investigate the conversion of ammonia-nitrogen. We also studied the effects of H_2O_2 and common ions (such as Mg^{2+}, Ca^{2+}, K^+, Na^+, SO_4^{2-}, NO_3^-, HCO_3^-/CO_3^{2-}, and Cl^-) present in

environmental water on the removal of ammonia-nitrogen. Furthermore, all tests were carried out at least twice, and the mean values are presented.

3. RESULTS AND DISCUSSION

The growth mechanism of the CdS-TiO_2 nanotube array on the AAO membranes using an electrochemical deposition strategy is presented below [27]:

$$2H_2O \rightarrow 2H^+ + 2OH^-$$

$$2H^+ + 2e^- \rightarrow H_2$$

$$S_2O_3^{2-} + 2e^- \rightarrow S^{2-} + SO_3^{2-}$$

$$S^{2-} + Cd^{2+} \rightarrow CdS$$

$$TiF_4 + (4-x)OH^- \rightarrow Ti(OH)_{4-x}F_x + (4-x)F^-$$

$$Ti(OH)_{4-x}F_x + xOH^- \rightarrow Ti(OH)_4 + xF^- \rightarrow TiO_2$$

At the primary reaction stage, hydroxyl ions were generated at a negative potential, which then diffused rapidly along the inner surface of the channels under the driving force of the electric field. The reaction was initiated by the diffusion of the $Ti(OH)_{4-x}F_x$ hydrolysate into these channels. On the other hand, TiO_2 nanotubes were formed after the deposition of TiO_2 onto the channel surface. Meanwhile, the reaction between the electrons and $S_2O_3^{2-}$ ions in the electrolyte was observed, along with the diffusion and reaction of S^{2-} ions with Cd^{2+}.

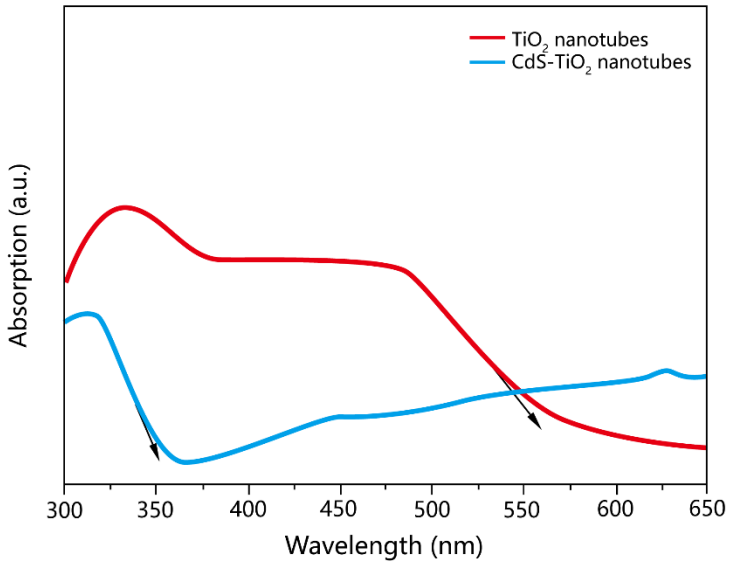

Figure 1. UV–visible absorption spectra (UV) of the TiO_2 and CdS-TiO_2 nanotubes.

As a result, CdS nanoparticles nucleated and grew. The sequential deposition of TiO_2 generated nanotubes, whereas the deposition of CdS generated discrete nanoparticles, since the Cd and S precursors had low concentrations. With continual electrochemical deposition, the thickness of the

TiO_2 nanotube shells and the diameter of CdS nanoparticles enlarged, causing CdS nanoparticles to be partially embedded in the shells of TiO_2 nanotubes. Eventually, the CdS-TiO_2 nanotube array was yielded after the removal of the AAO membrane using a NaOH solution (1 M).

The original TiO_2 nanotube array and CdS-TiO_2 nanotube array were characterized via absorption spectra, as shown in Fig. 1. The former primarily absorbed UV light (wavelength: < 350 nm), while the latter showed an extended band edge into the visible region (wavelength: *ca.* 580 nm). The TiO_2 nanotubes were likely effectively sensitized by the CdS nanoparticles.

Potentiostatic (current vs time, *I*–*t*) experiments were performed under intermittent illumination to study the photoresponse of the as-prepared CdS-TiO_2 nanotube array. The *I*–*t* profile was plotted under a −0.3 V bias (Fig. 2). In addition, the obtained CdS-TiO_2 nanotube array electrode exhibited much higher photocurrent compared with the original TiO_2 nanotube electrode. In comparison to the open-circuit photovoltage (Voc) for the plain TiO_2 nanotube array electrode, the Voc increased for the prepared CdS-TiO_2 nanotube array electrode. The short-circuit photocurrent of the CdS-TiO_2 nanotube array electrode was higher than that of the plain TiO_2 nanotube array electrode [28-31]. In addition, the former electrode rapidly generated photocurrent under intermittent illumination, suggesting fast charge transport.

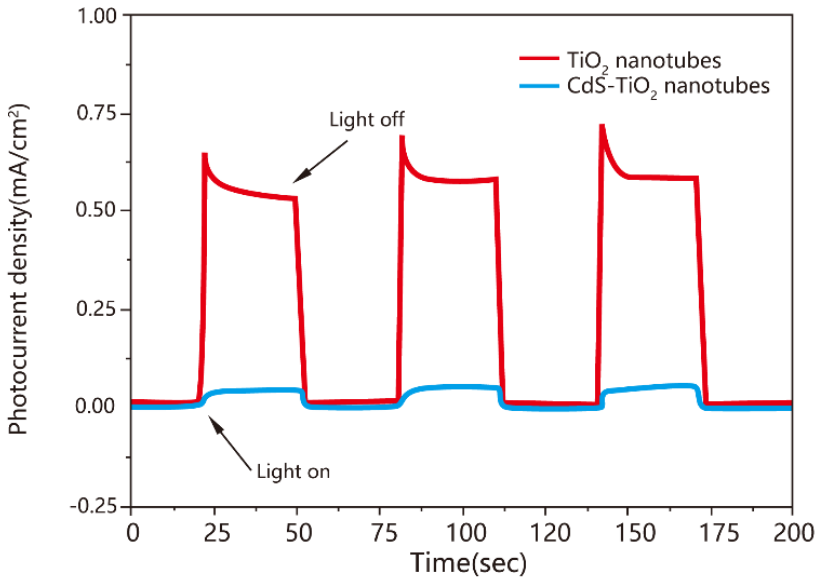

Figure 2. Photocurrent dynamics of the TiO_2 nanotube array and CdS-TiO_2 nanotube array when exposed to on–off light irradiation (wavelength of light: 365 nm).

With the aforementioned one-stage electrodeposition strategy, in addition to CdS, other semiconductors with narrow bad gaps could be utilized for the sensitization of TiO_2 nanotubes. CdTe- and CdSe-nanoparticle-sensitized TiO_2 nanotube arrays were prepared in this work. The photocatalytic activities of the as-prepared hybrids were studied by a range of control tests. In addition, the pH and catalyst amount were the same for all the tests, approximately 10 and 1 g/L, respectively. Meanwhile, a mercury lamp (500 W) was used throughout the experiments. The corresponding results are shown in Fig. 3. After reaction for 5 h, ca. 15% removal of ammonia-nitrogen was achieved via two approaches.

The first one was direct photolysis, and the second route was magnetically stirring and then escaping from the reaction solution. Meanwhile, more than 50% removal of ammonia-nitrogen was achieved after the photocatalytic degradation using the catalyst. With respect to CdS-TiO_2, the maximum removal efficiency of ammonia-nitrogen was 67.2%.

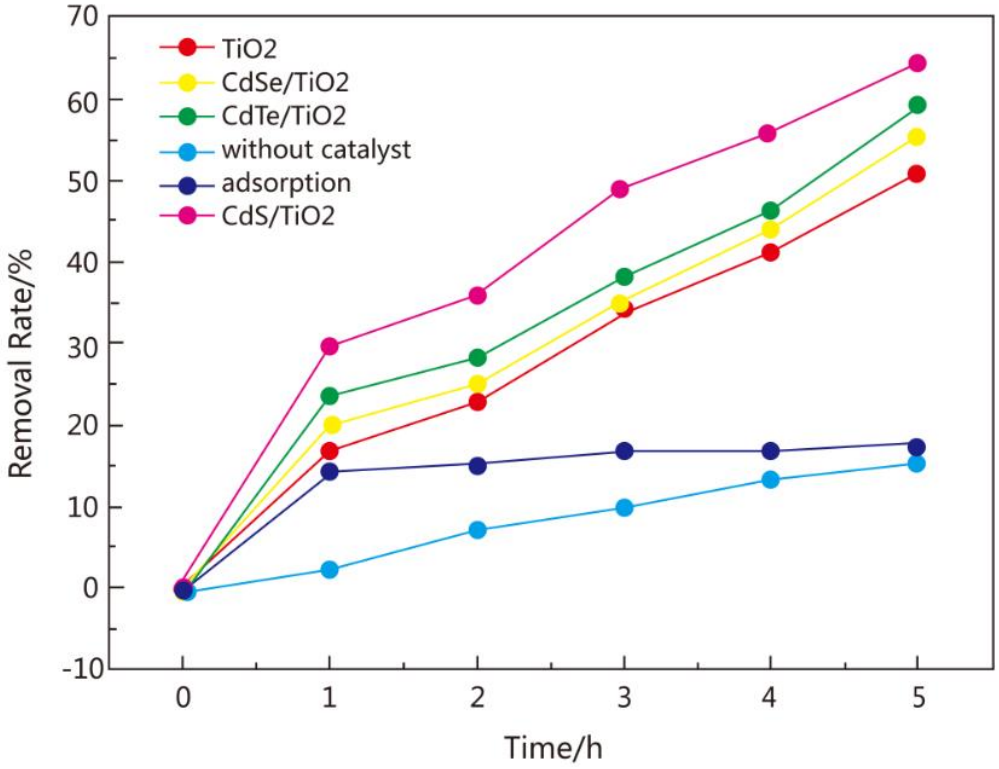

Figure 3. The photocatalytic profiles of NH_4^+-N degradation using TiO_2, CdSe/TiO_2, CdTe/TiO_2, and CdS/TiO_2 as catalysts.

The removal efficiency of ammonia-nitrogen was affected by the existing form of ammonia-nitrogen in water, and the surface charge of CdS-TiO_2 was affected by the initial pH value of the reaction solution. Initially, an increase in OH^- was observed with a gradual increase in the pH value, and an increased ammonia-nitrogen removal rate was caused by an increasing number of CdS-TiO_2-induced ·OH species. Then, ammonia-nitrogen existed in the following forms in water: NH^{4+} and $NH_3{\cdot}H_2O$. An increase in the proportion of $NH_3{\cdot}H_2O$ species was observed with an increase in the solution pH. In addition, NH_3 presents less steric hindrance compared with NH_4^+, which allows for a faster reaction of NH_3 with ·OH. However, the catalytic reaction exhibited no changed at a pH of 10.9 (Fig. 4) possibly because OH^- existed excessively in the aforementioned solution. A pH of approximately 10 was selected for the subsequent tests. It is obvious that the CdS/TiO_2 nanocomposite exhibited a considerable enhancement of the photocatalytic activity. The mechanism of the enhanced performance can be explained as follows. It is well known that fast recombination of photoinduced charge carriers is a main problem restricting the photocatalytic performance of TiO_2. The electrons produced from the valence band of TiO_2 can be transferred to the CdS nanoparticles. Therefore, the electron-hole pair recombination can be highly reduced. Then, these electrons can reduce oxygen and

form O_2^- ions. Finally, the O_2^- ions can react with H_2O and form •OH radicals, which degrade NH_4^+-N [32].

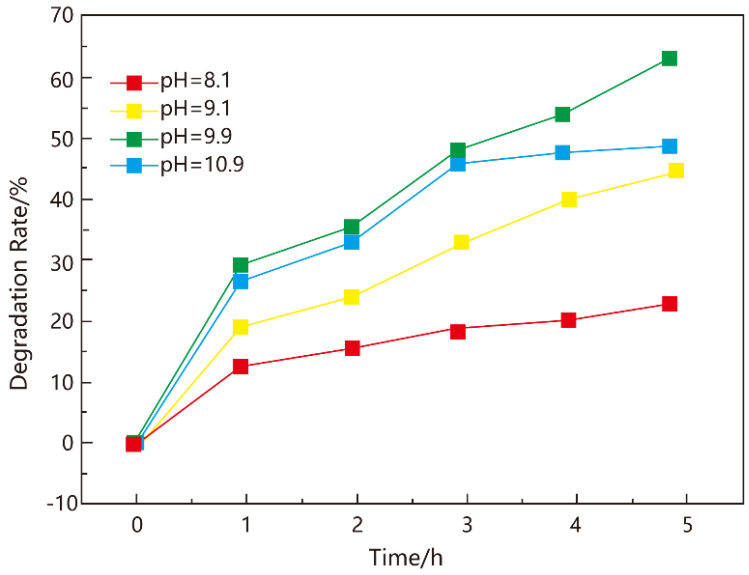

Figure 4. The effect of pH value on the degradation performance of NH^{4+}-N using CdS-TiO_2 as catalyst.

Ordinarily, eight inorganic ions exist in environmental water: HCO_3^-/CO_3^{2-} (0.1 mM), NO_3^- (0.1 mM), SO_4^{2-} (0.1 mM), Cl^- (0.1 mM), Mg^{2+} (0.1 mM), Ca^{2+} (0.1 mM), K^+ (0.1 mM), and Na^+ (0.1 mM). The removal of pollutants in water may be influenced by these ions. Fig. 5 demonstrates the effects of anions and cations on the degradation of ammonia-nitrogen, where a considerable inhibition effect for all the inorganic ions (under the same test conditions) on the removal of ammonia-nitrogen was observed. The pollutant degradation rate during the reaction decreased after adding NO_3^-. In addition, an increase in the inhibition effect was observed with a prolonged reaction, possibly due to the excessive NO_3^- generated through the conversion of ammonia-nitrogen. Note that the corresponding content will be presented below. A unique inhibitory effect of HCO_3^-/CO_3^{2-} was shown on the CdS-TiO_2-induced ammonia-nitrogen degradation. SO_4^{2-} and Cl^- also reacted with ·OH, similar to HCO_3^-/CO_3^{2-}, showing lower reaction capacities compared with NO_3^- and smaller inhibition effects compared with HCO_3^-/CO_3^{2-}. The inhibition capacity of doubly charged SO_4^{2-} may be higher compared with Cl^-.

Mg^{2+}, Ca^{2+}, K^+, and Na^+ are all in their most stable and highest oxidization states, unable to capture holes or electrons in the solution. We presume that no obvious effect is observed for the above metal ions on the CdS-TiO_2-induced ammonia-nitrogen photodegradation. The inhibitory effects of the above ions on the removal of ammonia-nitrogen are shown in Fig. 5B, due to the Cl^- ions that also existed in solution. These metal ions were added in the form of chloride salts. Based on these results, the photodegradation may be inhibited by Cl^- ions during its reaction with ·OH. Na^+ and K^+ exhibited similar characteristics because they belong to the same elemental main group.

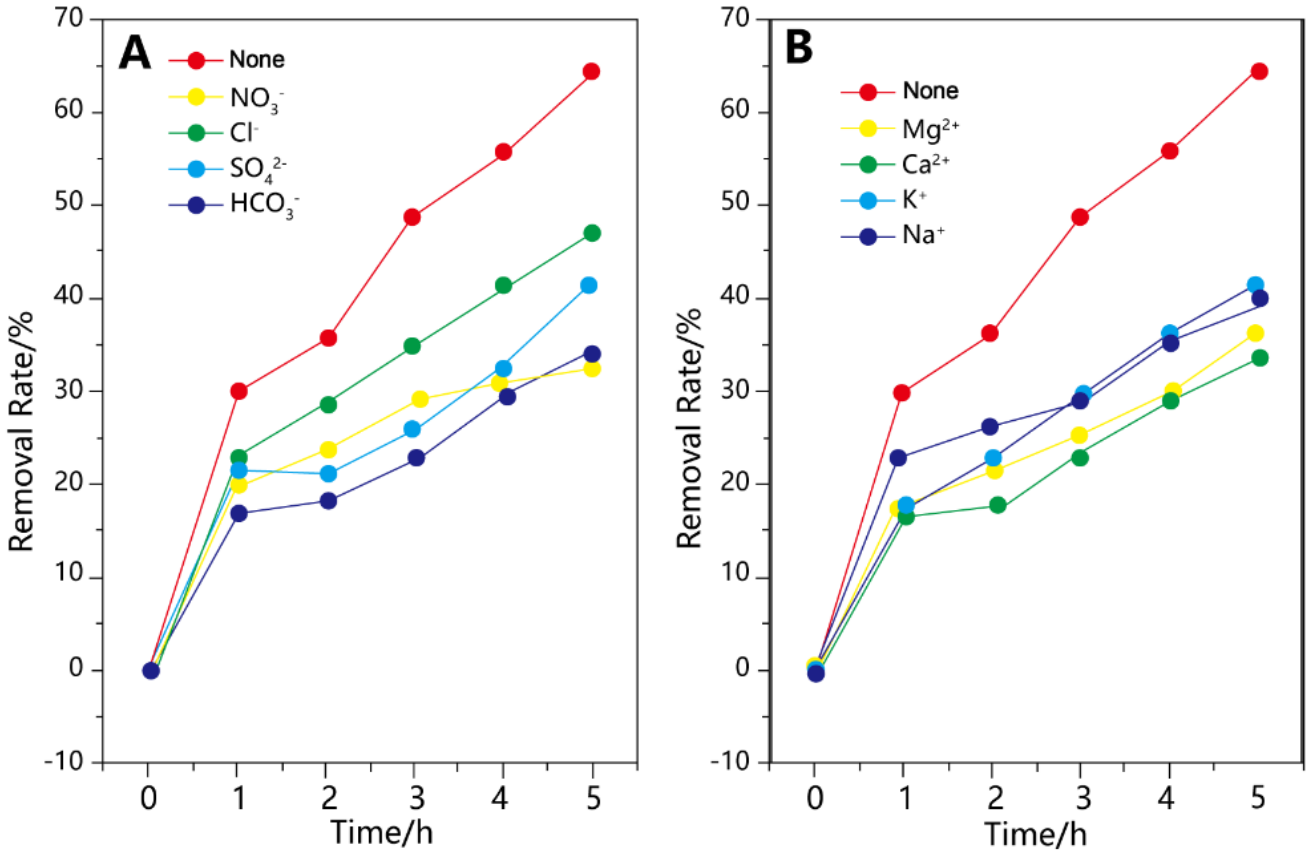

Figure 5. The effects of interference ions on the degradation of NH^{4+}-N using CdS-TiO_2 as a catalyst.

4. CONCLUSIONS

This work fabricated a CdS-TiO_2 nanotube array using a one-stage electrodeposition strategy, and compared this array with other CdS-TiO_2 nanotube arrays. Our developed CdS-TiO_2 nanotube array had the capacity of harvesting solar light not only in the UV region but also in the visible-light region up to 580 nm. In addition to CdS, a TiO_2 nanotube arrays sensitized by other semiconductor nanoparticles were also prepared in this work. A TiO_2-based nanostructure was prepared using a common, one-stage electrodeposition route. By comparison, the photocatalytic degradation capacity of CdS-TiO_2 to ammonia-nitrogen wastewater was more desirable. Furthermore, inhibition effects on ammonia-nitrogen degradation were shown by all ordinary inorganic ions in water.

References

1. H. Yu, L. Xu, P. Wang, X. Wang and J. Yu, *Appl. Ctatl. B-Environ.*, 144 (2014) 75.
2. A. Alshameri, A. Ibrahim, A. Assabri, X. Lei, H. Wang and C. Yan, *Powder Technology*, 258 (2014) 20.
3. D. Qu, D. Sun, H. Wang and Y. Yun, *Desalination*, 326 (2013) 135.

4. R. Iwata, T. Yamauchi, Y. Hirota, M. Aoki and T. Shimazu, *Applied Thermal Engineering*, 72 (2014) 244.
5. M. Altomare and E. Selli, *Catalysis Today*, 209 (2013) 127.
6. H. Yuzawa, T. Mori, H. Itoh and H. Yoshida, *J Phys Chem C*, 116 (2012) 4126.
7. W. Mook, M. Chakrabarti, M. Aroua, G.A. Khan, B. Ali, M. Islam and M. Hassan, *Desalination*, 285 (2012) 1.
8. M. Altomare, G. Chiarello, A. Costa, M. Guarino and E. Selli, *Chem. Eng. J.*, 191 (2012) 394.
9. W. Qian, . Greaney, S. Fowler, S. Chiu, A. Goforth and J. Jiao, *ACS Sustainable Chemistry & Engineering*, 2 (2014) 1802.
10. Y. Lai, J. Huang, H. Zhang, V. Subramaniam, Y. Tang, D. Gong, L. Sundar, L. Sun, Z. Chen and C. Lin, *J. Hazard. Mater.*, 184 (2010) 855.
11. Y. Kuo, T. Su, F. Kung and T. Wu, *J. Hazard. Mater.*, 190 (2011) 938.
12. H. Wang, Y. Su, H. Zhao, H. Yu, S. Chen, Y. Zhang and X. Quan, *Environmental Science & Technology*, 48 (2014) 11984.
13. Y. Liu, Y. Li, W. Li, S. Han and C. Liu, *Appl. Surf. Sci.*, 258 (2012) 5038.
14. Y. Ohko, I. Ando, C. Niwa, T. Tatsuma, T. Yamamura, T. Nakashima, Y. Kubota and A. Fujishima, *Environmental Science & Technology*, 35 (2001) 2365.
15. E. Grabowska, J. Reszczyńska and A. Zaleska, *Water. Res.*, 46 (2012) 5453.
16. T. Ochiai and A. Fujishima, *J Photoch Photobio C*, 13 (2012) 247.
17. R. Daghrir, P. Drogui and D. Robert, *Ind. Eng. Chem. Res.*, 52 (2013) 3581.
18. A. Linsebigler, G. Lu and J. Yates Jr, *Chemical Reviews*, 95 (1995) 735.
19. R. Asahi, T. Morikawa, T. Ohwaki, K. Aoki and Y. Taga, *Science*, 293 (2001) 269.
20. J. Yu, L. Zhang, Z. Zheng and J. Zhao, *Chemistry of Materials*, 15 (2003) 2280.
21. X. Chen, L. Liu, Y. Peter and S. Mao, *Science*, 331 (2011) 746.
22. S. Kumar and L. Devi, *The Journal of Physical Chemistry A*, 115 (2011) 13211.
23. K. Obata, K. Kishishita, A. Okemoto, K. Taniya, Y. Ichihashi and S. Nishiyama, *Appl. Ctatl. B-Environ.*, 160 (2014) 200.
24. M. Reli, N. Ambrožová, M. Šihor, L. Matějová, L. Čapek, L. Obalová, Z. Matěj, A. Kotarba and K. Kočí, *Appl. Ctatl. B-Environ.*, 178 (2015) 108.
25. M. Altomare, M. Dozzi, G. Chiarello, A. Di Paola, L. Palmisano and E. Selli, *Catalysis Today*, 252 (2015) 184.
26. J. Liu, B. Liu, Z. Ni, Y. Deng, C. Zhong and W. Hu, *Electrochimica Acta*, 150 (2014) 146.
27. Z. Shao, W. Zhu, Z. Li, Q. Yang and G. Wang, *J Phys Chem C*, 116 (2012) 2438.
28. B. Sun, T. Shi, X. Tan, Z. Liu, Y. Wu and G. Liao, *Materials Today: Proceedings*, 3 (2016) 443.
29. J. Lee, S. Makuta, S. Sukarasep, J. Bo, T. Suzuki, T. Nakayama, H. Suematsu, K. Niihara and Y. Tachibana, *Journal of Photopolymer Science and Technology*, 29 (2016) 357.
30. M. Zhang, Z. Gong, J. Tao, X. Wang, Z. Wang, L. Yang, G. He, J. Lv, P. Wang and Z. Ding, *Journal of Nanoparticle Research*, 3 (2017) 1.
31. C. Vázquez, A. Baruzzi and R. Iglesias, *IEEE Journal of Photovoltaics*, 6 (2016) 1515.
32. L. Fu, Y. Zheng, Z. Fu, W. Cai and J. Yu, *Functional Materials Letters*, 8 (2015) 1550036.